# Barrier-traversal-time operator and the time-energy uncertainty relation

Denny Lane B. Sombillo* and Eric A. Galapon
*Theoretical Physics Group, National Institute of Physics, University of the Philippines, Diliman Quezon City 1101, Philippines*

(Received 4 March 2018; revised manuscript received 29 May 2018; published 27 June 2018)

A general barrier-traversal-time operator is constructed using the time-of-arrival formalism. We study the operator's dynamics and determine the role played by the time-energy commutation relation. It turns out that similar dynamics is observed whether the traversal-time operator is canonically conjugate to the system Hamiltonian or not. We also use the barrier-traversal-time operator to calculate the traversal-time distributions for different cases (free case, and above-the-barrier and under-the-barrier traversals). The peak of the traversal-time distributions coincides with the classical expected traversal times for the free case and the above-the-barrier case. We then present our interpretation of the time-energy uncertainty relation that is consistent with the different traversal-time distributions.

DOI: 10.1103/PhysRevA.97.062127

## I. INTRODUCTION

Understanding the role of time in quantum mechanics has become more relevant since the advent of attosecond tunneling-time measurement [1–4]. Different proposals to calculate the tunneling time are introduced which claim to agree with the experimental results [5–11]. Nevertheless, some works are critical to the assumptions made in the original attoclock experiment [12] which are essential in the interpretation of tunneling-time calculation.

Measurement using the attoclock experiment suggests that tunneling time is probabilistic in nature and calculation of a time distribution is far more important than the mean time value [13]. In the standard formulation of quantum mechanics, we often associate an operator to a probability distribution. However, due to the famous Pauli objection on the issue of the time operator, many attempted to calculate a time-observable distribution using an alternate route [14,15], one of which is the use of a Bohmian trajectory to calculate the mean traversal time [16–18]. In the Bohmian-trajectory approach, the probability current is used to calculate the time-of-arrival (TOA) distribution. In [19], we cited a specific example where the probability current failed to reproduce the expected TOA distribution. This motivates us to reconsider the operator approach in the calculation of a barrier-traversal-time distribution.

Another interesting issue in the quantum time problem is how to interpret the time-energy uncertainty relation (TEUR). It must be emphasized that the TEUR does not share the same solid interpretation as the position-momentum uncertainty relation [15]. Despite this, some works presuppose that the time factor in the TEUR is the traversal time itself and the energy part is the uncertainty in the energy within the traversal region [9,10]. Suppose we presuppose that all observables, including time, can be associated with an operator. What interpretation of the TEUR is consistent with the time probability distribution obtained using the operator formalism?

We use the theory of quantized time-of-arrival operator [20–22] to construct a barrier-traversal-time operator. This is done by extracting the classical traversal time from the arrival time difference between two identical wave packets, one of which encounters a barrier and the other traverses an unobstructed region [23]. We then introduce the barrier-traversal-time operator by removing the initial wave function from the traversal-time expectation value. Upon doing this, we are left with an operator with no physical interpretation. The physical meaning of a time operator can be obtained from its dynamics [24]. This is done by evolving the eigenfunctions of the time operator using the Schrödinger equation. Given an arbitrary initial wave function, one can now calculate the traversal-time distribution using the spectral decomposition of the operator. Using the traversal-time distribution for different incident wave packets, we can now determine the interpretation of the time-energy uncertainty relation that is consistent with operator formalism.

This paper is organized as follows: In Sec. II we introduce the theory of the quantum time-of-arrival operator and demonstrate how the operator dynamics can be used to interpret a specific time observable. In Sec. III we construct a barrier-traversal-time operator using the basic idea laid down in [23]. In Sec. IV we investigate the barrier-traversal-time operator dynamics to interpret the traversal-time eigenvalue. In Sec. V we calculate the barrier-traversal-time distribution for different cases and evaluate the possible interpretation of the TEUR. In Sec. VI the barrier-traversal-time operator is used to study the tunneling case. Finally, we conclude in Sec. VII.

## II. QUANTUM TIME-OF-ARRIVAL OPERATOR

In this section we give a summary of how to obtain the operator corresponding to a time observable given its classical form. There are two ways to obtain a time operator. The first one is to straightforwardly apply a certain quantization rule on the classical observable without considering the time-energy canonical commutation relation (TECCR) while the second one is to start with the TECCR. These two approaches will yield

*dsombillo@nip.upd.edu.ph

 

identical results provided that the potential energy function gives a linear classical equation of motion.

### A. Quantization of classical TOA

The time interval at which a particle reaches a given point in space given its initial position is calculated by inverting the classical equation of motion. Let $H(q,p)$ be the classical system Hamiltonian. It follows that, at some arbitrary point $q'$ of the particle's trajectory, we have

$$H(q,p) = \frac{\mu}{2}\left(\frac{dq'}{dT}\right)^2 + V(q'), \tag{1}$$

where $V(q')$ is the potential energy function, $\mu$ is the particle's mass, $q$ is the initial position, and $p$ is the initial momentum. If we set $q = X$ to be the arrival point, then we can interpret $T = T(q,p)$ as the classical TOA of a particle with initial position $q$ and initial momentum $p$. Inverting Eq. (1), we get

$$T(q,p) = -\mathrm{sgn}(p)\sqrt{\frac{\mu}{2}}\int_X^q \frac{dq'}{\sqrt{H(q,p)-V(q')}}. \tag{2}$$

The factor $-\mathrm{sgn}(p)$, where $\mathrm{sgn}(p)$ is the sign function, fixes the sign of the arrival time $T(q,p)$; i.e., if the particle moves toward the arrival point then $T$ is positive and if the particle moves away from $X$ then $T$ is negative.

The quantization of $T(q,p)$ must be restricted to the trajectories that pass through the arrival point $X$ and to the first arrival of the particle [20]. This is done by taking the expansion of the integral in the neighborhood of the arrival point in the form $T(q,p) = \sum_{k=0}^{\infty}(-1)^k T_k(q,p)$, where $T_k$'s are determined recursively through

$$\begin{aligned} T_0(q,p) &= -\mu(q-X)p^{-1}, \\ T_k(q,p) &= -\mu p^{-1}\int_X^q \frac{\partial V}{\partial q'}\frac{\partial T_{k-1}}{\partial p}dq'. \end{aligned} \tag{3}$$

This leads to the form $T(q,p) = \sum_{m,n\geqslant 0}\alpha_{m,n}q^n p^{-m}$, where $\alpha_{m,n}$ are determined by the specific form of $V(q)$. Using the Weyl quantization rule, we have the operator

$$\begin{aligned} \mathbf{T} &= \sum_{m,n\geqslant 0}\alpha_{m,n}\mathbf{T}_{m,n}, \\ \mathbf{T}_{m,n} &= 2^{-n}\sum_{j=0}^{n}\binom{n}{j}\mathbf{q}^j\mathbf{p}^{-m}\mathbf{q}^{n-j}. \end{aligned} \tag{4}$$

Here, $\mathbf{q}$ and $\mathbf{p}$ are now the representation-free position and momentum operators, respectively. The action of the TOA operator $\mathbf{T}$ on an arbitrary wave function $\varphi(q)$ is determined by taking the position representation of the vector $\mathbf{T}|\varphi\rangle$:

$$\mathbf{T}\varphi(q) = \int_{-\infty}^{+\infty}\frac{\mu}{i\hbar}T(q,q')\mathrm{sgn}(q-q')\varphi(q')dq' \tag{5}$$

with kernel factor $T(q,q')$ given by

$$T(q,q') = \frac{1}{2}\int_0^{\eta} {}_0F_1\left(1;\frac{\mu}{2\hbar^2}\zeta^2\{V(\eta)-V(s)\}\right)ds, \tag{6}$$

where ${}_0F_1$ is a specific hypergeometric function, and $\zeta = (q-q')$, $\eta = (q+q')/2$. For the free-particle case where $V(q) = 0$, the kernel is simply $T_F(\eta,\zeta) = \eta/2$.

For the case of a rectangular potential barrier of width $w$ and height $V_0$ such that $V(q) = V_0 > 0$ in $-w-\epsilon \leqslant q \leqslant -\epsilon$ and zero elsewhere, the kernel factor takes the form

$$T_B(\eta,\zeta) = \begin{cases} \frac{\eta}{2} - \frac{w}{2}[J_0(\kappa|\zeta|)-1], & \eta < -w-\epsilon \\ \frac{\eta}{2} - \frac{\epsilon}{2}[I_0(\kappa|\zeta|)-1], & -w-\epsilon \leqslant \eta \leqslant -\epsilon \\ \frac{\eta}{2}, & -\epsilon \leqslant \eta, \end{cases}$$

where $\kappa = \sqrt{2\mu V_0/\hbar^2}$ with $I_0(x)$ and $J_0(x)$ as the modified and unmodified Bessel functions of the first kind of order zero, respectively. In the subsequent discussion, we let $\epsilon = 0$ since the $\epsilon$ term also introduces a delay when the particle traverses the free region from the transmission edge of the barrier to the arrival point [25]. Hence, the effective kernel can now be written as

$$T_B(\eta,\zeta) = T_F(\eta,\zeta) - (w/2)[J_0(\kappa|\zeta|)-1]H(-\eta-w), \tag{7}$$

where $H(x)$ here is the Heaviside step function.

### B. Algebra preserving time-of-arrival operators

The quantization of $T(q,p)$ does not guarantee that the constructed operator satisfies the required TECCR. One has to go beyond quantization to uphold the required commutation relation. This approach is fully described in [21] with all the technical details. We summarize the essential steps in this section. First, we assume an integral form for the TOA operator given in Eq. (5). Next we impose the TECCR; i.e., for $|\tilde{\varphi}\rangle, |\varphi\rangle \in \mathcal{H}$, where $\mathcal{H}$ is the system's Hilbert space with $\mathbf{H}$ as the Hamiltonian and $\mathbf{T}$ the TOA operator given in Eq. (5), we have

$$\langle\tilde{\varphi}|[\mathbf{H},\mathbf{T}]|\varphi\rangle = i\hbar\langle\tilde{\varphi}|\varphi\rangle. \tag{8}$$

If we plug Eq. (5) into Eq. (8), we obtain a differential equation for the kernel factor $T(q,q')$:

$$\begin{aligned} -\frac{\hbar^2}{2\mu}\frac{\partial^2 T(q,q')}{\partial q^2} + \frac{\hbar^2}{2\mu}\frac{\partial^2 T(q,q')}{\partial q'^2} \\ + (V(q)-V(q'))T(q,q') = 0, \end{aligned} \tag{9}$$

subject to $T(q,q) = q/2$ and $T(q,-q) = 0$. Solving Eq. (9) using power series in $(q-q')$ and $(q+q')$, one will obtain $T(q,q') = \sum_{k=0} T_k(q,q')$ where $T_0(q,q')$ is given by Eq. (6) and $T_{k\geqslant 1}(q,q')$ corresponds to the kernel factor that gives the quantum correction to the classical TOA [20]. If the potential energy function is given by $V(q) = aq^2 + bq + c$, where $a$, $b$, and $c$ are real numbers, then the result of Eq. (9) is the same as Eq. (6).

Imposing the TECCR requirement in Eq. (8) onto the TOA operator requires numerical analysis [26] since the general solution cannot always be closed analytically. In this work, we need an analytical form of $T(q,q')$ in the construction of a quantized barrier-traversal-time operator. Here we will use the quantized time-of-arrival operator whose kernel factor is given by Eq. (6).

### C. Dynamics of the quantized TOA operator

The quantum TOA operator has a well-known and expected dynamics [24,27]. That is, the operator eigenfunctions evolve into functions with singular support at the arrival point at

the time equal to the corresponding eigenvalues. Two distinct dynamics are common to all quantum TOA operators: these are the non-nodal and the nodal unitary collapse. The non-nodal collapse corresponds to particle detection at the arrival point while the nodal corresponds to nondetection [19]; that is, one will always have a collapse in all measurements whether one ends up detecting the particle or not. These dynamics are also present in the quantized TOA operator with a potential barrier. If we construct the time operator in Eq. (5) using the kernel in Eq. (7) and solve the eigenvalue problem, we can obtain the corresponding eigenfunctions. Some of these eigenfunctions, in the form of position probability distributions, are shown in Fig. 1(a). Now, we evolve the eigenfunctions of the quantum TOA operator using the Schrödinger equation and we obtain the corresponding dynamics shown in Figs. 1(b) and 1(c). Notice the distinct features of these dynamics. Both eigenfunctions give rise to a distribution with minimum position uncertainty around the arrival point at the time equal to the TOA operator eigenvalue. If the distribution is nonzero at the arrival point and has a minimum uncertainty around that point, then we can interpret that as a particle appearance [19,27].

The TOA operator that gives us the dynamics in Fig. 1 does not satisfy the required commutation relation with the system Hamiltonian. However, if we let the barrier height approach zero in Eq. (7), we obtain a TOA operator that satisfies the TECCR. Evolving the eigenfunctions of this free TOA operator gives a similar dynamics in Fig. 1. This might suggests that the unitary dynamics is independent on the TECCR but in [22] it was shown that there are cases when nonunitary collapse is observed when quantization does not satisfy the TECCR. The similarity between the dynamics of the quantized TOA and the TECCR-satisfying case is essential in our attempt to interpret the meaning of the TEUR.

## III. CONSTRUCTION OF THE BARRIER-TRAVERSAL-TIME OPERATOR

One possible way to determine the time interval that takes a particle to cross a region is to place a detector at the entry point to record the entry time and place another detector at the exit point to record the exit time. This means that one has to perform two time measurements to obtain the traversal time. The problem with this scheme is that the entry point detector will already collapse the wave function of the incident particle even before it enters the region. To avoid altering the actual wave-function propagation, we use an indirect traversal-time-measurement scheme.

Consider the setup where a detector $D_T$ is located at the origin to announce the arrival of a particle and a detector $D_R$ is located at the far left of the origin. A potential barrier $V(q)$ with width $w$ is placed between $D_T$ and $D_R$ such that the right edge of the barrier is located at the origin. A localized wave packet $\psi(q)$ is prepared between $D_R$ and the barrier at $t = 0$. The TOA is recorded when $D_T$ clicks; otherwise, no data are collected when $D_R$ clicks. This is repeated a large number of times, with the same initial state for every repeat. The average TOA at $D_T$ is then computed. Now, consider a second setup with the same set of detectors but without the barrier. The average free time of arrival at $D_T$ is computed from the new TOA data. The two average arrival times are then compared. This indirect

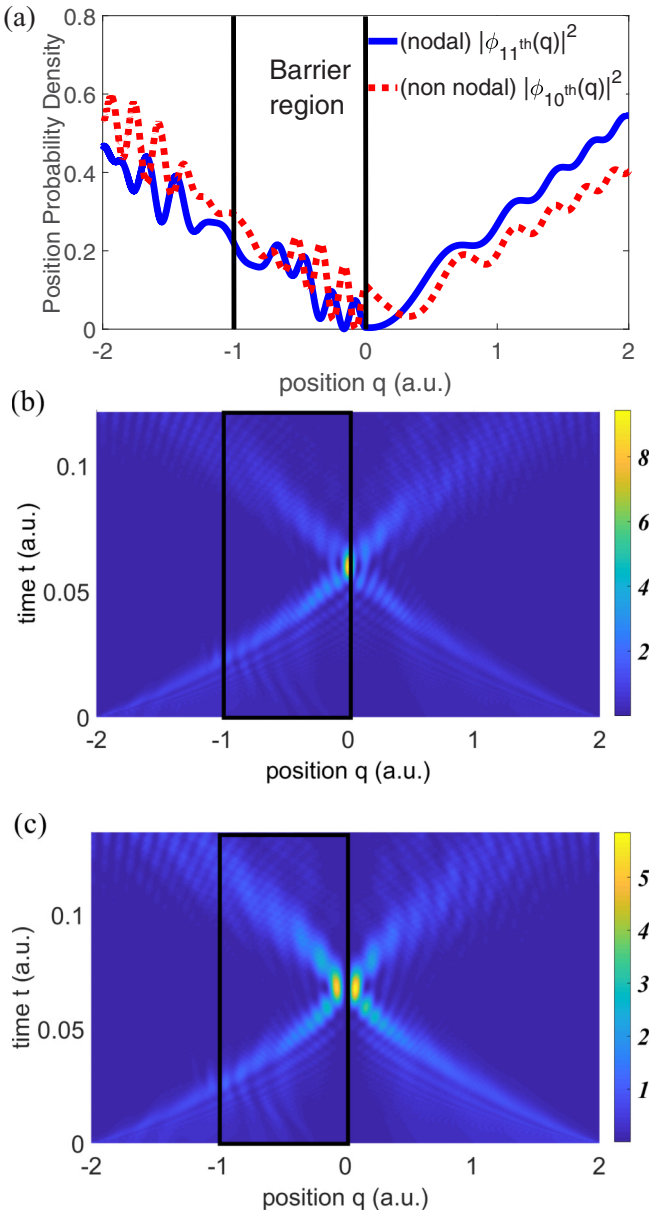


FIG. 1. Dynamics of the quantum time-of-arrival operator for the potential barrier with height $V_0 = 1.00$ and width $w = 1.00$. The vertical lines mark the boundaries of the barrier along the position axis. (a) The position distribution of the 10th- and the 11th-largest eigenvalue eigenfunction with respective eigenvalues of $\tau_{10} = 0.06058$ and $\tau_{11} = 0.06840$. (b) Time evolution of the $|\phi_{10\text{th}}(q,t)|^2$. (c) Time evolution of $|\phi_{11\text{th}}(q,t)|^2$.

traversal-time measurement is similar to the photonic tunneling experiment in [28]. Note, however, that the difference between the free arrival time and the arrival time in the presence of the barrier is not itself the barrier-traversal time.

In terms of the expectation values of the two arrival-time operators, we have

$$\Delta\tau = \langle\psi|\mathbf{T_F}|\psi\rangle - \langle\psi|\mathbf{T_B}|\psi\rangle,$$

where $\mathbf{T_F}$ is the free TOA operator and $\mathbf{T_B}$ is the TOA operator for the barrier potential. Our initial state $\psi(q)$ has a momentum expectation value of $\hbar k_0$ and takes the form

$\psi(q) = \varphi(q)e^{-ik_0 q}$, where $\langle\varphi|\mathbf{p}|\varphi\rangle = 0$. Using Eq. (5) and the corresponding kernel, the TOA difference $\Delta\tau$ takes the form

$$\Delta\tau = \frac{w\mu}{\hbar k_0}\mathrm{Im}(Q^* - R^*) \tag{10}$$

with

$$Q^* = k_0\int_0^\infty d\zeta\, e^{ik_0\zeta}\,\Phi(\zeta),$$
$$R^* = k_0\int_0^\infty d\zeta\, e^{ik_0\zeta}\,\Phi(\zeta)J_0(\kappa\zeta),$$

where $\Phi(\zeta) = \int_{-\infty}^{+\infty} d\eta\bar{\varphi}(\eta - \frac{\zeta}{2})\varphi(\eta + \frac{\zeta}{2})$ and $J_0(x)$ is the Bessel function of the first kind of order zero.

Consider now the classical limit of the TOA difference $\Delta\tau$, i.e., $\hbar \to 0$. It was shown by one of us in [23] that $\mathrm{Im}Q^* \to 1$. This implies that the first term in Eq. (10) approaches the free traversal time of a particle that covers a distance $w$ with velocity $\hbar k_0/\mu$. Similarly, the classical limit gives $\mathrm{Im}R^* \to k_0/k'$, where $k' = \sqrt{k_0^2 - \kappa^2}$ is the reduced wave number in the barrier region. Notice that $\mathrm{Im}R^*$ plays the role of an effective index of refraction and $\mu\mathrm{Im}R^*/\hbar k_0$ corresponds to the reduced velocity of the particle as it traverses the barrier region. This means that the second term in Eq. (10) gives the time to traverse the barrier region of width $w$ with the reduced velocity of $\hbar k'/\mu$.

Now, take the part of the TOA difference in Eq. (10) that corresponds to a particle's classical traversal time in the barrier region as $\hbar \to 0$ and interpret it as an expectation value of some temporal operator. The classical limit suggests that this operator correspond to the barrier-traversal-time observable. We now assume that the barrier-traversal-time operator $\mathcal{T}$ is also an integral operator in position representation; i.e., for a given wave function $\psi(q)$,

$$(\mathcal{T}\psi)(q) = \int_{-\infty}^{+\infty}\frac{\mu}{i\hbar}T_{\mathrm{trav}}(q,q')\mathrm{sgn}(q-q')\psi(q')dq' \tag{11}$$

with the kernel

$$T_{\mathrm{trav}}(q,q') = \frac{w}{2}J_0(\kappa|\zeta|)H(-\eta - w). \tag{12}$$

This assumption is justified since $\mathcal{T}$ is derived from the time-of-arrival operator expectation value. The kernel $T_{\mathrm{trav}}(q,q')$ was obtained by isolating the term in the TOA difference that corresponds to the barrier-traversal time in the classical limit. Notice that the operator $\mathcal{T}$ does not really require the initial wave function to have an incident energy above the barrier height. Thus, we can use $\mathcal{T}$ both for over-the-barrier traversal and for the tunneling case.

## IV. DYNAMICS OF THE BARRIER-TRAVERSAL-TIME OPERATOR

Suppose we are presented with an operator given in Eq. (11) with kernel in Eq. (12). How do we know what observable this operator represents? A physical meaning can be attached to the barrier-traversal-time operator by exploring its dynamics, similar to what we have done to the TOA operator [19,24]. We calculate first its eigenvalues and eigenfunctions which requires solving a Fredhold integral equation of the second kind. We do this by following a coarse-graining procedure done in [27]. That is, we confine the system in a segment of length $2l$ centered at the transmission edge of the barrier. The eigenvalue problem is solved numerically using the Clenshaw-Curtis method [29]. We set $l = 2$, $\hbar = \mu = V_0 = w = 1$, and use $N = 3001$ points to discretize the segment $[-l,+l]$. The barrier-traversal-time operator becomes a $3001 \times 3001$ matrix operator. The eigenvalues and eigenfunctions of this operator are obtained using the IMSL 7.0 package `EVCCG_INT`.

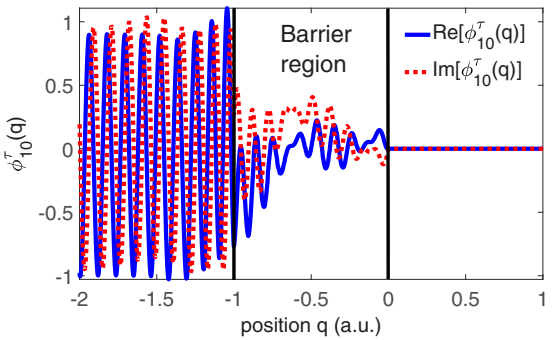


FIG. 2. The tenth-largest-eigenvalue eigenfunction of the barrier-traversal-time operator for $V_0 = 1$.

For a given value of $V_0$, the resulting eigenfunctions can be classified into three. Half of the eigenfunctions have zero eigenvalue while the other half have either positive or negative eigenvalues. The positive-eigenvalue and the negative-eigenvalue eigenfunctions have zero value in the transmission side (see Fig. 2). The signs of their corresponding eigenvalues can be associated to their respective propagation under the time-evolution operator; i.e., positive-eigenvalue eigenfunctions generally propagate toward the positive direction and negative-eigenvalue eigenfunctions propagate toward the negative direction. However, the zero-eigenvalue eigenfunctions are Dirac-$\delta$-like functions with singular support located in the transmission side.

It suffices to consider only the positive-eigenvalue eigenfunctions of the $\mathcal{T}$ in extracting the quantum-mechanical meaning of traversal. Figure 3(a) shows the position density distribution of the tenth-largest-eigenvalue eigenfunction of the barrier-traversal-time operator. At this point, we assume that the initial wave packet has already collapsed into one of the eigenfunctions of $\mathcal{T}$. Notice that the support of the eigenfunction's position distribution at some initial time zero is in the interval $q \in [-l,0)$. This appropriately describes a particle's wave function with initial position peak in the left side of the barrier and possibly having a nonvanishing support inside the barrier region. We evolve the eigenfunction in Fig. 3(a) using the Schrödinger equation. The result is shown in Fig. 3(b). Notice that the position probability density propagates to the right and crosses the barrier after some time. This implies that the positive-eigenvalue eigenfunctions are composed mainly of positive momentum components. Figure 3(b) also shows that the part of the positive-eigenvalue eigenfunction that is inside the barrier region propagates in the opposite direction. Furthermore, at the time equal to the eigenvalue, most of the position probability density is already inside the barrier region. This is further illustrated in Fig. 3(c), where we obtain the probability of finding the particle in three

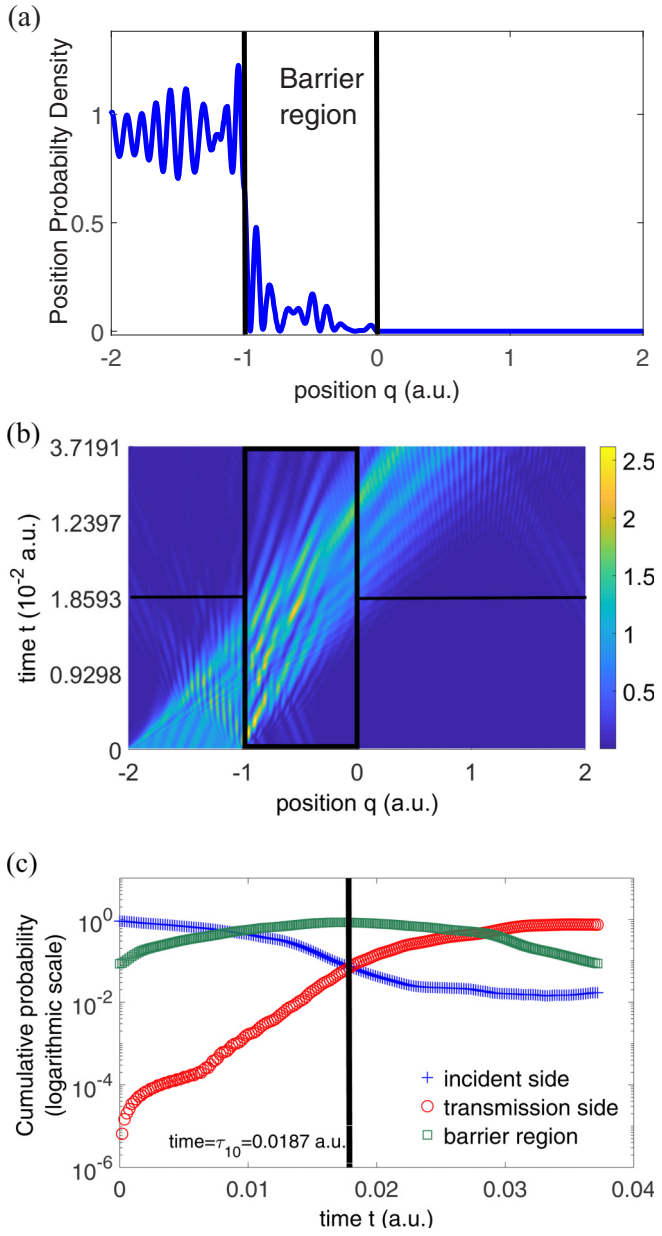


FIG. 3. Dynamics of the barrier-traversal-time operator for a barrier with height $V_0 = 1$. (a) The position distribution of the tenth-largest-eigenvalue eigenfunction of the barrier-traversal-time operator with eigenvalue $\tau = 0.0187$. (b) The time-evolved position distribution of (a). The vertical rectangle represents the barrier region and the horizontal line corresponds to the eigenvalue time. (c) The cumulative probabilities of finding the particle in the incident (blue +), the transmission (red ○), and the barrier (green □) regions.

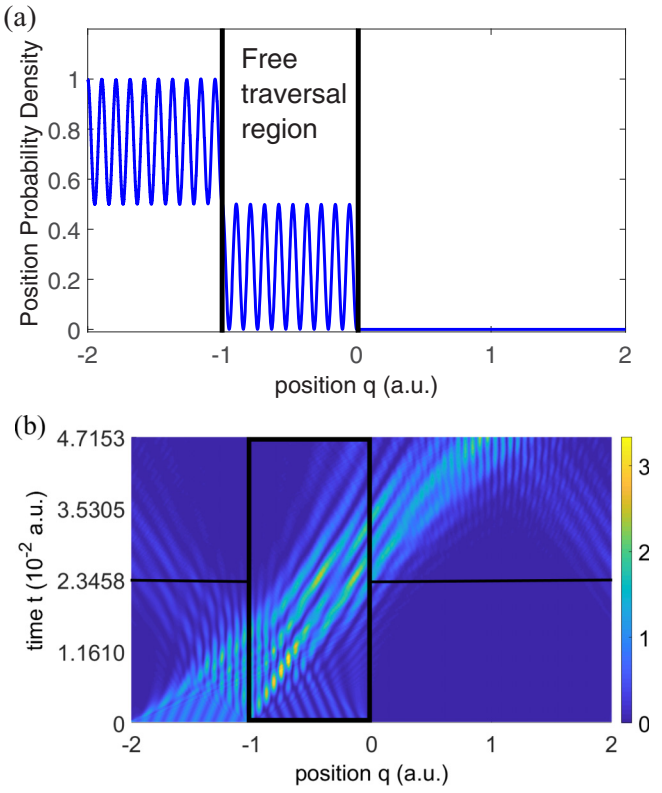


FIG. 4. Dynamics of the free traversal time operator ($V_0 = 0$). (a) The position distribution of the tenth-largest-eigenvalue eigenfunction of the free-traversal-time operator with eigenvalue $\tau = 0.023458$. (b) The time-evolved position distribution of (a). The vertical rectangle represents the traversal region and the horizontal line corresponds to the eigenvalue time.

different regions (the incident side, the barrier region, and the transmission side). We see that the time corresponding to the instant when the particle is most likely to be found inside the barrier region is in the neighborhood of the eigenvalue time. Note that in the construction of the barrier-traversal-time operator we require two time measurements, so the eigenvalue time that we obtain should be interpreted as a time interval. Thus, we can now say that the barrier-traversal-time operator measures the time interval at which the particle is most likely to be found in the barrier region.

One possible contention to the physical interpretation that we attach to the barrier-traversal-time operator is that the constructed operator does not satisfy the required commutation relation and the dynamics in Fig. 3 could be misleading. We can address this by letting the barrier height approach zero. If we set $V_0 = 0$ [equivalently $\kappa = 0$ in Eq. (12)], the resulting free-traversal-time kernel reduces to

$$T_{\text{trav}}(q,q') = \frac{w}{2} H(-\eta - w). \tag{13}$$

One can easily check that the kernel in Eq. (13) satisfies Eq. (9) for $V(q) = 0$ and therefore the free-traversal-time operator is canonically conjugate to the free Hamiltonian.

We can now check if different dynamics is exhibited by this canonical free-traversal-time operator. The position distribution of one of the free-traversal-time operators is shown in Fig. 4(a). Note that the sharp transition in the position distribution of the free-traversal-time operator eigenfunction is due to the Heaviside function in Eq. (13) and not because of the presence of the barrier. The way we construct the barrier-traversal-time operator in Sec. III isolates a particular region of space which manifests as a Heaviside function in the kernel. Figure 4(b) shows the time evolution of the eigenfunction in Fig. 4(a). The dynamics of the free case in Fig. 4(b) is similar

to that of the barrier case in Fig. 3(b). This similarity implies that the same physical interpretation can be attached to the TECCR-satisfying $\mathcal{T}$ operator and the TECCR-violating $\mathcal{T}$ operator.

## V. TRAVERSAL-TIME DISTRIBUTION AND THE TEUR

With the knowledge of what observable the operator in Eq. (11) with kernel Eq. (12) represents, we can now proceed to the calculation of the barrier-traversal-time probability density distribution and evaluate the meaning of the TEUR. The calculation of the probability distribution is done by using the spectral decomposition of $\mathcal{T}$. In all our numerical analysis we choose the familiar Gaussian wave packet as the initial state of our particle with mean kinetic energy $E_0 = \hbar^2 k_0^2/2\mu$ and initial momentum $\hbar k_0$. In the position representation our initial state is

$$\psi_0(q) = \left(\frac{1}{2\pi\sigma_q^2}\right)^{1/4} \exp\left[-\frac{(q-q_0)^2}{4\sigma_q^2} + ik_0 q\right], \quad (14)$$

where we set the initial position $q_0 = -5$ and the mass $\mu = 1$. The position variance and the incident energy of the initial state will be varied in the numerical experiment. Given the initial state $|\psi_0\rangle$, the traversal-time distribution is obtained using the Born rule:

$$P_{\psi_0}(t) = \sum_{\tau \leqslant t} |\langle \varphi^\tau | \psi_0 \rangle|^2, \quad (15)$$

where $\tau$ and $|\varphi^\tau\rangle$ are the $\mathcal{T}$-operator eigenvalue and eigenvector, respectively. Using the probability $P_{\psi_0}(t)$, the density distribution is obtained by differentiation with respect to time, i.e., $\partial P_{\psi_0}(t)/\partial t$. The peaks of the distribution determine the most likely value of the traversal time.

Our treatment is purely numerical in nature. First, we construct the operator $\mathcal{T}$ in a line segment $[-8,8]$ with 5001 Chebyshev points and solve the eigenvalue problem using the Clenshaw-Curtis method [29]. We then take the overlap of the initial state in Eq. (14) with each of the eigenvectors of $\mathcal{T}$ and generate the probability $P_{\psi_0}(t)$ in Eq. (15). Finally, we interpolate the probabilities and numerically calculate the derivative with respect to time to obtain the probability density. The calculated probability density will then be used to evaluate the meaning of the TEUR.

The precise form of the time-energy uncertainty relation is given by

$$\Delta E \Delta T \geqslant \frac{\hbar}{2}. \quad (16)$$

In this paper we consider four possible ways to interpret the TEUR:

(i) $\Delta E$ is the uncertainty in the incident energy and $\Delta T$ is the uncertainty in the traversal time.

(ii) $\Delta E$ is the effective mean energy in the traversal region and $\Delta T$ is the mean traversal time.

(iii) $\Delta E$ is the uncertainty in the incident energy and $\Delta T$ is the mean traversal time.

(iv) $\Delta E$ is the effective mean kinetic energy in the traversal region and $\Delta T$ is the uncertainty in the traversal time.

In the following discussions, we evaluate each interpretation using the traversal-time distribution. We focus first on the free- and the above-the-barrier-traversal cases where we can still use the classical expected traversal time in evaluating the TEUR.

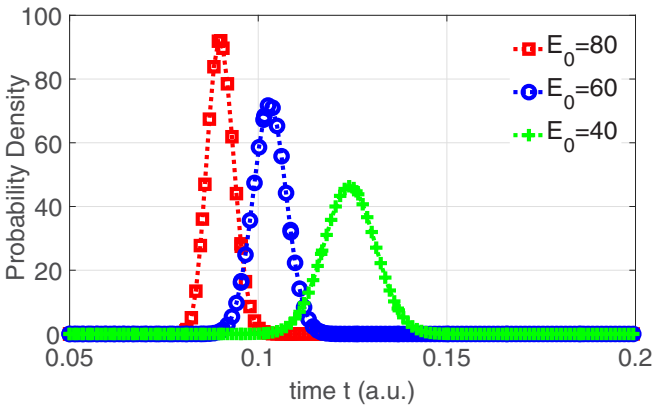


FIG. 5. Free-traversal-time distribution for different incident energies. The peak traversal times agree with the classical result $\tau_{\text{class}} = w/\sqrt{2\mu E_0}$.

### A. Free traversal

The free-traversal-time operator meets all the requirements that we want for a time operator, i.e., a definite dynamics consistent with our notion of traversal with expectation value that agrees with the classical result and an operator satisfying the TECCR. Figure 5 shows the different free-traversal-time distribution for incident wave packets having the same initial position variance but with different incident energies. One can easily verify that the traversal peak time of each distribution coincides with the classical result, i.e., $\tau_{\text{class}} = w\sqrt{\mu/2E_0}$. In addition, the eigenfunctions used to obtain Fig. 5 exhibit the dynamics that we show in Fig. 4. This means that the free-traversal-time distribution is directly tied to the dynamics of $\mathcal{T}$.

Let us consider the standard TEUR interpretation (i), where both the time and energy factors are interpreted as uncertainties. In Fig. 6, we set the mean incident energy to be $E_0 = 40$ and vary the position variance from $\sigma_q^2 = 0.25$ to $\sigma_q^2 = 1.00$.

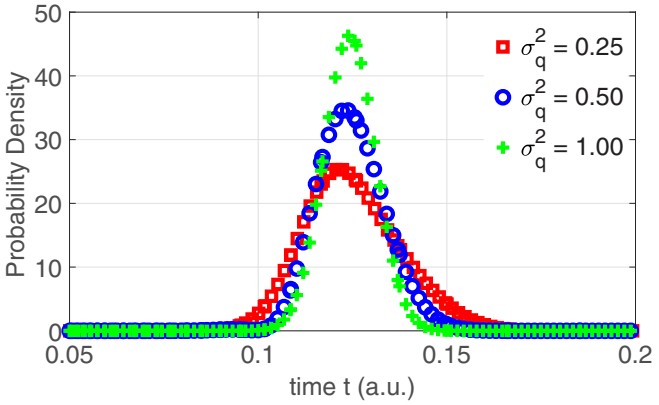


FIG. 6. Free-traversal-time distribution for different position variances with $E_0 = 40$. The width of the traversal-time distribution decreases as the incident energy width decreases.

Increasing the position variance will result in the narrowing of the incident energy width due to the position-momentum uncertainty relation. Notice that, as the energy width decreases (from red □ to blue ○ to green + in Fig. 6), the traversal-time uncertainty decreases as well. This is in direct contradiction with Eq. (16) if we insist that $\Delta E$ is the incident energy width and $\Delta T$ is the traversal-time uncertainty. Thus, interpretation (i) is not consistent with the traversal-time-operator formalism.

Take note that we have satisfied all the requirements needed by a time operator for the free case and we still do not end up with the standard TEUR interpretation (i). It is either that the operator formalism for time is wrong or the TEUR requires a different interpretation. It is hard to confront the latter since this suggests that quantization of a classical observable and a commutation relation are not enough in the construction of a quantum operator.

Consider the extreme case where the initial state is a plane-wave function. We have here a state of definite kinetic energy and therefore the energy width is zero. If we extrapolate the behavior in Fig. 6, then this means that the traversal-time uncertainty will reach a minimal value. Note that the width of the resulting traversal-time distribution cannot be zero since the only initial state that will give a definite traversal time is one of the free $\mathcal{T}$ eigenfunctions and these are not plane waves (see Fig. 4). Nevertheless, interpretation (i) of the TEUR is still violated since $\Delta E \Delta T = 0$.

For interpretation (ii) of the TEUR, one might argue that $\Delta T$ is already the traversal peak time in Fig. 5 and $\Delta E$ is the mean incident energy $E_0$. It is true that as we increase $E_0$, the traversal peak time decreases, i.e., the peak shifts to the left. However, a closer look into this interpretation reveals that this cannot be the case. Since the peak time of the distribution coincides with the classical traversal time then we can set $\Delta T = w\sqrt{\mu/2E_0}$. Interpretation (ii) of the TEUR now gives

$$\Delta T \Delta E = w\sqrt{\frac{\mu}{2E_0}}E_0 = wk_0\left(\frac{\hbar}{2}\right), \tag{17}$$

where we used $E_0 = \hbar^2 k_0^2/2\mu$. Notice that interpretation (ii) of the TEUR can only be satisfied if $wk_0 \geqslant 1$. But the width of the barrier, $w$, and the incident wave vector of the particle, $k_0$, are completely independent of each other. Thus, interpretation (ii) is not an implication of the operator formalism of traversal time.

We can readily dismiss interpretation (iii) of the TEUR since changing the energy width should not affect the traversal peak time. It is the mean kinetic energy that determines how fast a quantum particle crosses a traversal region. At this point, we are only left with interpretation (iv), where we treat $\Delta T$ as the uncertainty in the traversal-time distribution and $\Delta E$ as the effective mean energy in the traversal region. The results in Fig. 5 are consistent with this interpretation. Increasing $E_0$ results in a distribution with decreasing traversal-time width.

### B. Over-the-barrier traversal

We now turn to the case where the traversal-time operator does not satisfy the required TECCR. This time we use the kernel given in Eq. (12) with $V_0 > 0$. The resulting barrier-traversal-time operator is no longer canonically conjugate to the system's Hamiltonian. Nevertheless, the eigenfunctions of $\mathcal{T}$ for the barrier case exhibit similar dynamics as the free case and therefore we can still associate $\mathcal{T}$ with the traversal-time observable. We follow the same numerical construction of $\mathcal{T}$ as in the free case.

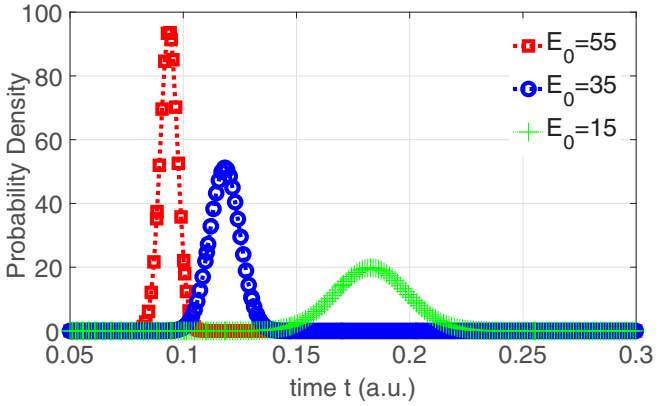


FIG. 7. Over-the-barrier-traversal time distribution for different incident energies. The peaks of the distribution are close to the classical result $\tau_{\text{class}} = w/\sqrt{2\mu(E_0 - V_0)}$.

Note that the barrier-traversal-time operator is independent of our incident wave packet. This means that we can use the numerically constructed $\mathcal{T}$ for the over-the-barrier traversal ($E_0 > V_0$) and the under-the-barrier case ($E_0 < V_0$). We start first with the over-the-barrier case. We use the same Gaussian wave packet in Eq. (14) as the initial state and the same procedure to calculate for the distribution. The parameters $V_0 = 5, w = 1, q_0 = -5$, and $\sigma_q^2 = 1$ are used, and the incident energy is varied. The result is shown in Fig. 7. For the over-the-barrier case, the traversal peak time of the distribution should still agree with the classical expected result since the particle can still classically traverse the barrier region. One can check that the peaks are close to $\tau_{\text{class}} = w/\sqrt{2\mu(E_0 - V_0)}$. In order to evaluate the possible interpretation of the TEUR we vary the initial position variance of the incident wave packet with mean energy of $E_0 = 15$. The result is shown in Fig. 8.

Let us now look into the interpretation of TEUR using the above-the-barrier traversal time distribution. Figure 8 is not

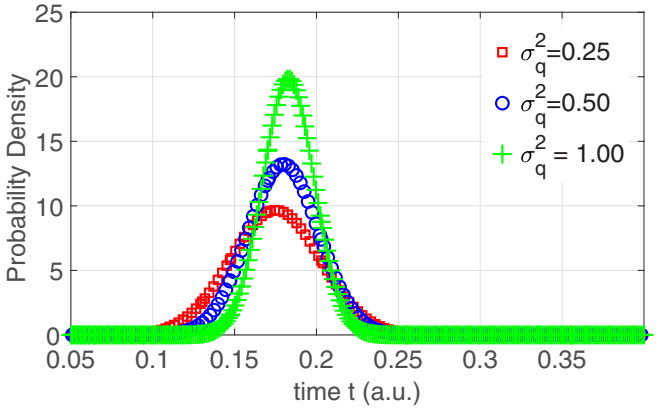


FIG. 8. Over-the-barrier-traversal time distribution for different initial position variance with $E_0 = 15$. The uncertainty in the traversal time decreases as the incident energy width decreases.

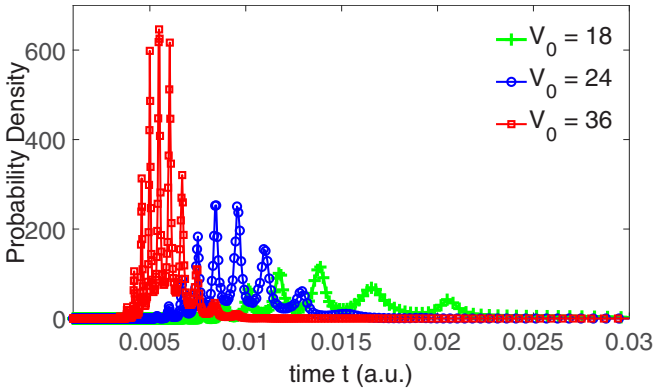


FIG. 9. Barrier-traversal-time distributions for different barrier height with fixed barrier width of $w = 1$ a.u. The incident wave packet used is a Gaussian function with incident energy of 8 a.u., initial position peak at $q = -5$ a.u., and initial position variance of $\sigma_q^2 = 1$ a.u.

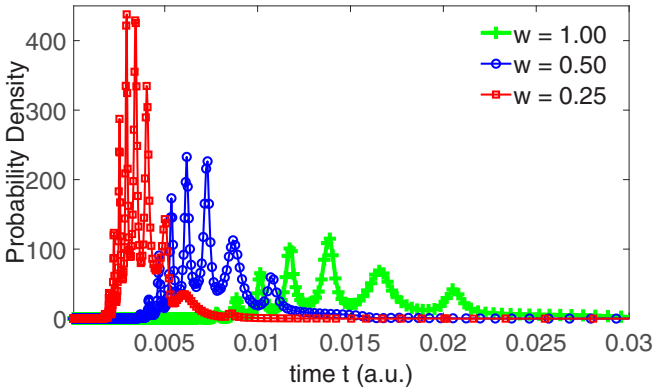


FIG. 10. Barrier-traversal-time distributions for different barrier width with fixed barrier height of $V_0 = 18$ a.u.- The incident wave packet used is a Gaussian function with incident energy of 8 a.u., initial position peak at $q = -4 - w$ a.u., and initial position variance of $\sigma_q^2 = 1$ a.u.

consistent with interpretation (i) for the same reason as the free case; i.e., the decreasing incident energy width results in decreasing traversal-time width. If we use the classical traversal-time value to estimate the peak time in Fig. 7, then interpretation (ii) will lead to a relation that involves a restriction among the independent parameters such as the barrier height, barrier width, and initial incident mean momentum of the incident wave packet. Thus, interpretation (ii) must also be abandoned. Interpretation (iii) is dismissed for the same reason as that of the free case. Finally, Fig. 7 suggests that only interpretation (iv) is consistent with the above-the-barrier-traversal case.

Here, we have seen that for the TECCR-satisfying $\mathcal{T}$ operator and for the TECCR-violating $\mathcal{T}$ operator the same interpretation of the TEUR emerged: $\Delta T$ is the uncertainty in the traversal-time distribution and $\Delta E = |E_0 - V_0|$ is the effective mean energy in the traversal region. In the next section we see that the same interpretation of the TEUR extends to the tunneling case.

## VI. APPLICATION TO TUNNELING: UNDER-THE-BARRIER TRAVERSAL

Tunneling can be considered by looking into the under-the-barrier-traversal case. Unlike the free and the over-the-barrier traversals, the under-the-barrier case can no longer be verified using the classical result. However, since the constructed operator is independent of the initial state, then we can still use it even for cases with no classical counterpart.

Consider again the initial Gaussian wave packet in Eq. (14). For numerical convenience, we vary the barrier height and fix the incident energy to $E_0 = 8$. We still set the centroid of the incident wave packet at $q = -5$ with variance of $\sigma_q^2 = 1$. The resulting distributions are shown in Fig. 9. Some minor comments are in order. The oscillations in the distribution are due to the finite-size effect of the confinement. The potential is effectively a finite square well and since the energy of the incident particle is less than the barrier height then some of the particle's energy component matches the energy bound states of the effective finite well. This results in resonance which manifests as multiple peaks in the distribution. The plots can be made smoother by making the confinement length very large.

Notice that the time corresponding to the traversal peak times of the distribution approaches zero as the barrier height increases. This is consistent with the result in [23], where only the above-the-barrier energy component of the incident particle contributes to any measurable tunneling-time delay. As the barrier height is increased, the energy component of the incident wave that is above the barrier becomes smaller, resulting in lower traversal time. The result of attoclock experiments stating that the tunneling time is nonzero despite being small is consistent with the distribution in Fig. 9. So long as the tunneling particle has an energy component that is above the barrier height, however small, the particle traverses the region in a nonzero time interval.

On a side note, in the attoclock experiment one can change the parameter of the barrier by changing the intensity of the incident pulse. The increase in the pulse intensity effectively decreases the height and narrows the effective width of the barrier. The changes in the distribution as the barrier height is changed are already shown in Fig. 9. However, it is the barrier width that is mostly affected by the change in the pulse intensity. In Fig. 10, we plot the barrier-traversal-time distribution as the barrier width is varied.

Notice that, as the width increases, the traversal peak time moves to higher values and the uncertainty becomes larger. This is similar to the tunneling-time distribution calculated in [2] using the Feynman path integral (FPI), where the tail of the distribution lengthens and the distribution peak position increases as the intensity of the pulse decreases. The FPI is used to interpret and provide a physical explanation of the attoclock tunneling-time experiment in [1]. Here, we have shown that one can obtain essentially the same result if we use the operator approach in the calculation of traversal-time distribution.

Let us go back and consider the TEUR in the under-the-barrier-traversal case. All the incident wave packets used in Fig. 9 have the same mean energies and energy width. Only the variation of the barrier height causes the peak traversal time and the traversal-time width to vary. This means that $\Delta E = |E_0 - V_0|$ for the under-the-barrier case. We have no

way to check if the peak traversal time will cause a possible violation of the TEUR. However, the independence of the barrier-traversal-time operator with the incident wave packet allows us to extend the interpretation that we have for $\Delta T$; i.e., it is the uncertainty in the traversal-time distribution. Knowing what the $\Delta T$ and $\Delta E$ in the TEUR represent will provide a reasonable estimate in improving the resolution of tunneling-time measurements [13].

## VII. CONCLUSION

We constructed a barrier-traversal-time operator using the quantized TOA operator. The dynamics of the barrier-traversal-time operator answers the question of what is happening to the quantum particle as it traverses the barrier region. That is, after the incident wave packet collapses into one of the eigenfunctions of the barrier-traversal-time operator the eigenfunction evolves such that the particle is most likely to be found in the barrier region after a time equal to the eigenvalue time. The dynamics of the eigenfunctions justify that the constructed operator measures the traversal time.

The constructed operator is applied to different traversal cases. For the free and the over-the-barrier traversals, the peak of the traversal-time distributions coincides with the classical expected result. The agreement with the classical result and the physical meaning provided by the dynamics justify the legitimacy of the traversal-time operator. We have also demonstrated that the tunneling time measured in the experiment is due to the above-the-barrier energy component of the incident particle. If the barrier height is increased, the above-the-barrier energy component of the particle gets smaller, resulting in a sharp traversal-time distribution with peak shifted towards lower values of time. The traversal time distribution for the tunneling case also agrees with the general behavior of the distribution used to simulate the attoclock tunneling experiment for different pulse intensities. Lower pulse intensity results in a broader barrier width, which lengthens the traversal-time distribution with peak located at larger values of time.

We also looked into the interpretation of the TEUR that is consistent with the barrier-traversal-time operator formalism. It turns out that the operator formalism suggests that $\Delta T$ is the width of the traversal time distribution and $\Delta E = |E_0 - V_0|$, where $E_0$ is the incident mean energy and $V_0$ is the effective barrier height. This means that the resolution of a traversal-time measurement is determined by how far is the mean energy of the traversing particle with respect to the potential height.

## ACKNOWLEDGMENTS

D.S. acknowledges the Office of the Chancellor of the University of the Philippines Diliman, through the Office of the Vice Chancellor for Research and Development, for funding support through the Thesis and Dissertation Grant (Project No. 151503 DNSE). This work was supported by the Department of Science and Technology through the National Research Council of the Philippines.

[1] P. Eckle, A. N. Pfeiffer, C. Cirelli, A. Staudte, R. Dörner, H. G. Muller, M. Büttiker and U. Keller, Science **322**, 1525 (2008).
[2] A. S. Landsman, M. Weger, J. Maurer, R. Boge, A. Ludwig, S. Heuser, C. Cirelli, L. Gallmann, and U. Keller, Optica **1**, 343 (2014).
[3] H. Ni, U. Saalmann, and J.-M. Rost, Phys. Rev. Lett. **117**, 023002 (2016).
[4] N. Camus, E. Yakaboylu, L. Fechner, M. Klaiber, M. Laux, Y. Mi, K. Z. Hatsagortsyan, T. Pfeifer, C. H. Keitel, and R. Moshammer, Phys. Rev. Lett. **119**, 023201 (2017).
[5] E. H. Hauge and J. A. Støvneng, Rev. Mod. Phys. **61**, 917 (1989).
[6] A. Landsman and U. Keller, J. Phys. B **47**, 204024 (2014).
[7] Z. Xiao and H. Huang, J. Math. Phys. **57**, 032102 (2016).
[8] T. Zimmermann, S. Mishra, B. R. Doran, D. F. Gordon, and A. Landsman, Phys. Rev. Lett. **116**, 233603 (2016).
[9] O. Kullie, J. Phys. B **49**, 095601 (2016).
[10] O. Kullie, Phys. Rev. A **92**, 052118 (2015).
[11] N. Teeny, C. H. Keitel, and H. Bauke, Phys. Rev. A **94**, 022104 (2016).
[12] L. Torlina, F. Morales, J. Kaushal, I. Ivanov, A. Kheifets, A. Zielinski, A. Scrinzi, H. Muller, S. Sukiasyan, M. Ivanov, and O. Smirnova, Nat. Phys. **11**, 503 (2015).
[13] A. S. Landsman and U. Keller, Phys. Rep. **547**, 1 (2015).
[14] *Time in Quantum Mechanics*, edited by J. G. Muga, R. Sala Mayato, and I. L. Egusquiza, Lecture Notes in Physics Vol. 374 (Springer, Berlin, 2008).
[15] A. Maquet, J. Caillat, and R. Taïeb, J. Phys. B **47**, 204004 (2014).
[16] C. R. Leavens, Phys. Lett. A **303**, 154 (2002).
[17] C. R. Leavens, Phys. Lett. A **345**, 251 (2005).
[18] N. Douguet and K. Bartschat, Phys. Rev. A **97**, 013402 (2018).
[19] D. B. Sombillo and E. A. Galapon, Ann. Phys. **364**, 261 (2016).
[20] E. A. Galapon, Int. J. Mod. Phys. A **21**, 6351 (2006).
[21] E. A. Galapon, J. Math. Phy. **45**, 3180 (2004).
[22] E. A. Galapon and J. P. Magadan, arXiv:1804.03344.
[23] E. A. Galapon, Phys. Rev. Lett. **108**, 170402 (2012).
[24] R. C. F. Caballar and E. A. Galapon, Phys. Lett. A **373**, 2660 (2009).
[25] D. L. Sombillo and E. A. Galapon, Phys. Rev. A **90**, 032115 (2014).
[26] D. B. Sombillo and E. A. Galapon, J. Math. Phys. **53**, 043702 (2012).
[27] E. A. Galapon, Proc. R. Soc. A **465**, 71 (2009).
[28] A. M. Steinberg, P. G. Kwiat, and R. Y. Chiao, Phys. Rev. Lett. **71**, 708 (1993).
[29] R. Vitancol and E. A. Galapon, Int. J. Mod. Phys. C **19**, 821 (2008).